The Berry Phase

Azure Hansen

Prof. Alfred Goldhaber
Physics 405: Advanced Quantum Physics
Stony Brook University

December 2006

1 Introduction

If you meet a friend who has just returned from vacation, the first two questions you ask him are "how long were you gone?" and "where did you go?" Equivalently, you may ask him "what is your dynamic phase?" and "what is your geometric phase?"

Geometric phase is interesting because it involves the often-neglected phase of the wavefunction, and because it is manifested in diverse fields of physics. This phase factor was first described generally by Sir Michael Berry in 1984 [1], but it had been observed in some forms before then [2].

Consider a system whose parameters are varied adiabatically and ultimately returned to their initial value. All systems acquire a phase factor during any time period, the dynamic phase. In some systems, the final state acquires in addition a geometric phase factor that depends on the geometry of the closed transit in parameter space of the evolution. Thus, the final state is not equivalent to the initial state due to the geometric, or Berry's, phase. This difference can be revealed through interference with a reference state. A system exhibiting geometric phase is termed nonholonomic.

An example of geometric phase from classical physics is that of a man walking slowly around the globe with a pendulum, always swinging the pendulum orthogonal to his direction of motion [3]. He begins at the North Pole walking southward. When he reaches the Equator, he turns and walks along it for a time, then turns north and ends where he began. There is a non-zero angle, the Hannay angle [4], between the pendulum axis in the initial and final states due to the geometric phase. In quantum mechanics, an example of Berry's phase is the Aharonov-Bohm effect involving a charged particle in an electric or magnetic field [5].

Here we explore the geometric phase in classical, quantum and optical systems. The phenomenon is especially interesting in optics due to the inherent similarities between quantum mechanical wavefunctions and electromagnetic waves.

2 Geometric phase in quantum mechanics

Many quantum mechanical systems exhibit a behavior that can be interpreted as a geometric phase. An example is the quantum Hall effect [**?**]. A geometric phase occurs in systems only where the Hamiltonian H itself is rotated; rotation of Ψ is has no interesting geometric effect.

Evolution of H can cause an observable change in Ψ. The path in parameter space must be closed so we can compare the original state to the final, via an interference.

2.1 Berry's derivation of geometric phase

In retrospect, it is amazing that the geometric phase was not discovered until 1984 with the publication of Berry's "Quantal phase factors accompanying adiabatic changes." In quantum systems the geometric phase is often called the Berry phase. The geometric phase arises only when there is a rotation of the Hamiltonian; rotation of the wavefunction Ψ produces familiar non-geometric results.

To study the geometric phase, we vary the parameters R of the Hamiltonian with time, then bring them back to their original value such that $R(t=0) = R(T)$. The Schrödinger equation is

$$H(R(t))|\Psi(t)\rangle = \imath\hbar|\dot{\Psi}(t)\rangle,$$

and the eigenstates must satisfy

$$H(R)|n(R)\rangle = E_n(R)|n(R)\rangle.$$

Berry showed [1] that the state $|n(R(t=0))\rangle$ will evolve as

$$|\Psi(t)\rangle = e^{-\imath\Phi_d(t)}\, e^{\imath\gamma_n(t)}\, |n(R(t))\rangle.$$

Here Φ_d is the familiar dynamic phase

$$\Phi_d = \frac{1}{\hbar}\int_0^t \mathrm{d}t' E_n(R(t')),$$

and $\gamma_n(t)$ is the geometric phase of interest.

Berry considers a spin particle in an adiabatically-varying magnetic field; here we consider the simple case of precession of the magnetic field about $\hat{z}$. The magnetic field direction is parallel to $\hat{n}$, and the spin particle to $\vec{\sigma}$. Varying parameter R rotates $\hat{n}$ by a tiny angle $\mathrm{d}\phi$ about $\hat{z}$

In each interval $\mathrm{d}t$, $\hat{n}$ shifts by a tiny angle to $\hat{n} + \mathrm{d}n$, such that we can assume that $\hat{n}$ is still parallel to $\hat{n} + \mathrm{d}n$. Thus the magnitude of $\langle n|\nabla_R n\rangle$ can not change, so it must be an imaginary phase term. The time derivative of $\gamma_n(t)$ must also depend on the time derivative of $R(t)$. We can then accept Berry's equation [1]

$$\dot{\gamma}_n(t) = \imath\langle n(R(t))|\nabla_R n(R(t))\rangle\dot{R}(t).$$

For a closed path in parameter space C from $t = 0$ to $t = T$, the geometric phase change in $|\Psi\rangle$ is

$$\gamma_n(C) = \imath \oint_C \langle n(R)|\nabla_R n(R)\rangle \cdot \mathrm{d}R.$$

Note that the dynamic phase is independent of C; it depends only on T. In three dimensions, this expression for γ can be related to the solid angle Ω enclosed by the path C.

We can also understand the geometric phase by imagining the path traced out by the Hamiltonian H in parameter space to be composed of many infinitesimal loops. The Hamiltonian is perpendicular to the plane of each infinitesimal loop, and its matrix is diagonal. Since the H is varied adiabatically, there can be no angle between H's at successive points. But when we sum over all these little loops, we get off-diagonal terms in H that manifest physically as a phase.

2.2 Aharonov-Bohm effect

The classic example of Berry's phase in a quantum mechanical system is the Aharonov-Bohm effect, where a particle is affected by fields in regions that it is forbidden from entering [5]. Consider an electron moving in a closed path around a long solenoid. The magnetic field from the solenoid is uniform through the center and zero outside it. However, the magnetic vector potential is non-zero outside the solenoid. The electron acquires a geometric phase from its trip, which be observed through electron interference. We will not go into detail on this system here; see [8].

3 Geometric phase in classical mechanics

Berry's 1984 derivation was specific to quantum systems, but geometric phase can be used to understand a great variety of systems, including classical ones. The dynamic phase in classical mechanics can be interpreted as a time-delay in a harmonic oscillator. As in quantum mechanics, the classical geometric phase then arises from an adiabatic change in the system parameters.

3.1 Foucault pendulum

A Foucault pendulum is a common display in science museums. It is named for its discoverer, 19th century French physicist Jean Bernard Léon Foucault; he also invented the gyroscope. A very long pendulum swings suspended over the center of a disk surrounded by blocks. The pendulum's vertical swinging axis precesses due to the motion of the Earth, and the pendulum knocks over the blocks periodically. This system is treated in a purely classical manner using either the Coriolis force, or by interpreting the system's behavior as a geometric phase.

In a uniformly rotating coordinate system, the equation of motion is generally

$$m\frac{d^2\vec{r}}{dt^2} = \vec{F} - 2m\vec{\omega} \times \frac{d\vec{r}}{dt} + m\vec{\omega} \times (\vec{\omega} \times \vec{r}),$$

where the last two terms are the coriolis and centrifugal forces, respectively, and ω is the frequency of rotation of the Earth.

The equation of motion for the Foucault pendulum [6], choosing the coordinates such that the origin is at the pendulum's rest (equilibrium) point, is

$$m\frac{d^2\vec{r}}{dt^2} = (\vec{\tau} + m\vec{g}) - 2m\vec{\omega} \times \frac{d\vec{r}}{dt} + m\vec{\omega} \times (\vec{\omega} \times \vec{r}), \tag{1}$$

where τ is the tension in the string, m is the mass of the bob, ω is the frequency of rotation of the Earth, g is the acceleration due to gravity, and r is such that $\vec{z}$ points outward from the center of the Earth and $\vec{x}$ and $\vec{y}$ describe the coordinates on the surface of the Earth.

We now assume that the frequency of oscillation of the pendulum ω_0 is large compared to the earth: $\omega_0 \gg \omega$; and ω_0 is small : $\dot{z} \approx 0$. We can therefore neglect the centrifugal force

because it is of order ω^2. Now our equations of motion are

$$\frac{d^2x}{dt^2} = -\omega_0^2 x + 2\frac{dy}{dt}\omega_z$$

$$\frac{d^2y}{dt^2} = -\omega_0^2 y + 2\frac{dx}{dt}\omega_z,$$

where $\omega_z = \omega\cos\theta$ and θ is the constant polar coordinate of the pendulum. We define a complex variable $\mathrm{w} \equiv x + \imath y$ and the equations of motion become

$$\frac{d^2\mathrm{w}}{dt^2} + 2\imath\omega_z\frac{d\mathrm{w}}{dt} + \omega_0^2\mathrm{w} = 0.$$

Solutions are of the form $\mathrm{w} = e^{\imath at}$, and we find

$$a = -\omega_z \pm \sqrt{\omega_z^2 + \omega_0^2} \approx -\omega_z \pm \omega_0.$$

So our equation of motion for the pendulum is

$$\mathrm{w}(t) = e^{\imath\omega_z t}\left(c_1 e^{\imath\omega_0 t} + c_2 e^{-\imath\omega_0 t}\right).$$

Therefore, we see that the coriolis force rotates the plane of oscillation of the pendulum with frequency ω_z. The geometric phase Φ_g is the phase acquired from this process [7]:

$$\Phi_g = \omega_z T = 2\pi\cos\theta, \tag{2}$$

where $T = \frac{2\pi}{\omega} = 24\,\mathrm{hr}$.

The result (2) is indeed a geometric phase. Φ_g is independent of time, as it does not contain either the frequency of rotation of the Earth or that of the oscillation of the pendulum. It can be related to the solid angle Ω of its closed path C by

$$\mathrm{mod}(\Phi_g, 2\pi) = \Omega(C).$$

4 Geometric phase in optics

In quantum mechanics, the wavefunction Ψ describes the state and evolution of a system. The form of Ψ is so similar to that of the electric field vector $\vec{E}$ that it is instructive to exploit optics as a way to understand quantum mechanics. Schrödinger particles and photons can both interfere, diffract and more. In optics, four distinct manifestations of Berry's phase have been shown experimentally: spin-redirection, Pancharatnam, spin-squeezing and first-order Gaussian modes. Here we explore these geometric phases and some relatively simple experiments to observe them.

4.1 Pancharatnam geometric phase

Pancharatnam's study of light in absorbing biaxial crystals revealed interference fringes that depended strangely on linear polarizers [10]. This led him to think about the issues involved in interfering two beams of linearly polarized coherent light that are not necessarily of the same polarization. From this came the first geometric phase in optics, although it was not recognized as such until decades later. Pancharatnam's original paper provides the most accessible derivation of the geometric phase, entirely using basic geometry.

4.1.1 Poincaré sphere in polarization state space

The Poincaré sphere describes the states of polarized light in a convenient geometric way [11]. Points on the surface of a sphere of unit radius correspond to various polarizations, as in figure 1. The north (south) pole is right (left) circularly polarized light. The equator of the sphere therefore corresponds to a polarization with equal components of left and right circularly polarized light: linearly polarized light. Along the equator, the lines of longitude give the angle of linearly polarized light, with points on and opposite the prime meridian being antiparallel. The points between the equator and poles correspond to elliptically polarized light.

The Stokes parameters provide another way to describe the polarization of light. These four dimensionless quantities depend on the amplitudes of the orthogonal components, their phase difference, and the angle of the polarization ellipse. The Stokes parameters may be interpreted geometrically as a radius and three Cartesian coordinates, and related directly to the Poincaré sphere.

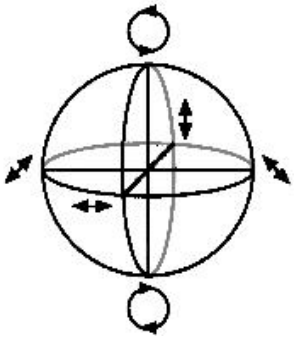

Figure 1: The Poincaré sphere representation of polarization states. [12]

One can easily describe the effect of an optical element or process using the Poincaré picture. Consider a system with the initial state of linearly polarized light, $\theta = \frac{\pi}{2}$, $\phi = 0$. After a quarter-wave plate operates on this state, it will become circularly polarized light, $\theta = \pi$, $\phi = 0$. The quarter-wave plate can then be referred to as a $\frac{\pi}{2}$ element.

This description of the states via the eigenstates of a system using a sphere is a very common practice; populations in a two-state atomic system are often described using the analogous Bloch sphere [13, 14]. A laser beam that transfers atoms entirely from the ground to the excited state is called a π pulse.

4.1.2 Pancharatnam's derivation

We will start with polarization state A on the Poincaré sphere, change it to B, then C, then bring it back to A, and see what happens.

Consider two laser beams polarized neither parallel or orthogonal to each other [10]. The two beams lie on the Poincaré sphere at points A and B, separated by the angle 2γ, as illustrated in figure 2. We can think of this situation as two electric field vectors $\vec{A}$ and $\vec{B}$ with an angle γ between them. Their intensities are $I_A = \vec{A}^2$ and $I_B = \vec{B}^2$, respectively. We can decompose $\vec{B}$ such that one of its components is parallel to $\vec{A}$.

$$\vec{A} = A_1\hat{1}, \vec{B} = B_1\hat{1} + B_2\hat{2}, \text{ where}$$

$$\hat{1} \perp \hat{2} \text{ and } \hat{1} \parallel \vec{A}$$

The intensity of each component of each beam is calculated.

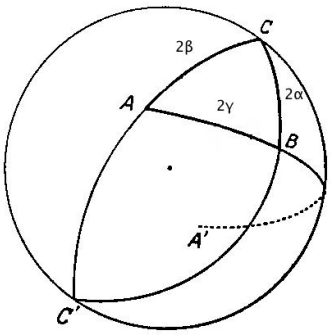

Figure 2: Poincaré sphere for Pancharatnam's derivation of the geometric phase. [10]

$$B_1 = B\cos\gamma, \;\; I_{B1} = I_B\cos^2\gamma$$

$$B_2 = B\sin\gamma, \;\; I_{B2} = I_B\sin^2\gamma$$

$$A_1 = A\cos\gamma, \;\; I_{A1} = I_A\cos^2\gamma$$

$$A_2 = 0, \;\; I_{A2} = 0$$

Now the $\hat{1}$- and $\hat{2}$-components of the total intensity are calculated.

$$I_1 = (A_1 + B_1)^2 = A_1^2 + B_1^2 + 2A_1B_1 = I_A + I_B + 2\sqrt{I_AI_B}\cos\gamma\cos\delta$$

$$I_2 = (A_2 + B_2)^2 = B_2^2 = I_B\sin^2\gamma$$

We have included a term $\cos\delta$ to account for any difference in phase between $A_1 = A$ and B_1. This will be important later.

So now the total intensity I_0 of the interference is

$$I_0 = I_1 + I_2 = I_A + I_B(\sin^2\gamma + \cos^2\gamma) + 2\sqrt{I_AI_B}\cos\gamma\cos\delta. \tag{3}$$

Now consider a beam of intensity I at the pole of the Poincaré sphere, point C, representing purely right circularly polarized light. In polarization state space, the angular separation of C and A (B) is 2β (2α). In the electric field vector picture, the angle between $\vec{C}$ and $\vec{A}$ is ($\vec{B}$) is β (α). Now, $\vec{C} = \vec{A} + \vec{B}$, where $\vec{A}$ and $\vec{B}$ are not necessarily orthogonal. We want to find I_B and I_A in terms of I, α, β and γ.

First, we again decompose each vector into $\hat{1}$- and $\hat{2}$-components such that $\hat{1} \parallel \vec{A}$.

$$\vec{A} = A_1\hat{1}, \;\; \vec{B} = B_1\hat{1} + B_2\hat{2}, \;\; \vec{C} = C_1\hat{1} + C_2\hat{2}$$

$$A_2 = 0, \;\; B_2 = B\sin\gamma, \;\; C_2 = C\sin\beta$$

$$C_2 = A_2 + B_2$$

$$C\sin\beta = B\sin\gamma$$

$$I_B = I\frac{\sin\beta^2}{\sin^2\gamma} \tag{4}$$

To find I_A, we use a system with coordinates $\hat{3}$ and $\hat{4}$, such that $\hat{3} \parallel \vec{B}$ and $\hat{3} \perp \hat{4}$.

$$\vec{A} = A_3\hat{3} + A_4\hat{4}, \;\; \vec{B} = B_3\hat{3}, \;\; \vec{C} = C_3\hat{3} + C_2\hat{4}$$

$$A_4 = A\sin\gamma, \;\; B_4 = 0, \;\; C_4 = C\sin\alpha$$

$$C_4 = A_4 + B_4$$

$$C\sin\alpha = A\sin\gamma$$

$$I_A = I\frac{\sin^2\alpha}{\sin^2\gamma} \tag{5}$$

Now we can use (5) and (4) in (3) to find the phase δ between the two beams A and B. Taking $I_0 = I$ and solving (3) for $\cos\delta$,

$$\cos\delta = (I_0 - I_A - I_B)/(2\sqrt{I_A I_B}\cos\gamma) = -(\sin^2\alpha + \sin^2\beta - \sin^2\gamma)/(2\sin\alpha\sin\beta\cos\gamma).$$

We also have $\alpha' = \alpha - \frac{\pi}{2}$, $\beta' = \beta - \frac{\pi}{2}$ and $\gamma' = \gamma$, so

$$\cos\delta = -\frac{\cos^2\alpha' + \cos^2\beta' + \cos^2\gamma}{2\cos\alpha'\cos\beta'\cos\gamma}, \tag{6}$$

where we have used the identity $1 = \cos^2\gamma + \sin^2\gamma$.

The surprising result is that geometrically, (6) is related to the solid angle Ω subtended by the triangle $C'BA$. The solid angle is in general given by the surface integral

$$\Omega = \int_S \sin\phi \, \mathrm{d}\phi\mathrm{d}\theta.$$

So for the phase between beams A and B we have

$$\delta = \pi - \frac{1}{2}\Omega. \tag{7}$$

We have thus obtained the geometric phase as derived by Pancharatnam in 1956. If the polarization state changes from A to B to C and back to A, the total phase is non-zero even if each state is in phase with the previous state.

4.1.3 Quantum mechanical derivation

Now we will derive Pancharatnam's phase using a more quantum-mechanical, and therefore more elegant, method [15, 16].

The polarization of a beam of light is given by

$$|\psi\rangle = \begin{bmatrix} \psi_+ \\ \psi_- \end{bmatrix},$$

$$\psi_\pm = \frac{1}{\sqrt{2}}(\epsilon_x \pm \epsilon_y),$$

where the complex unit vector is $\vec{\epsilon} = (\epsilon_x, \epsilon_y)$.

The phase difference $\Phi_{1,2}$ between states $|\psi_1\rangle$ and $|\psi_2\rangle$ is given by

$$\Phi_{1,2} = \arg(\langle\psi_1|\psi_2\rangle),$$

where arg is the complex argument. If two states have a real and positive scalar product, they are perfectly in phase.

Now we change the polarization state from 1 to 2, then 2 to 3, and finally 3 to 1. Each time, the phase of the new state is "in phase" with the previous state. The net phase is given by

$$\arg(\langle\psi_1|\psi_2\rangle\langle\psi_2|\psi_3\rangle\langle\psi_3|\psi_1\rangle),$$

which was shown by Pancharatnam to be $-\frac{1}{2}\Omega_{123}$, where Ω is the solid angle on the Poincaré sphere formed by the three polarization states.

4.1.4 Experiment

The Pancharatnam geometric phase involves a change in polarization state space, manifested as a change in the polarization vector of the system. Experimentally, this requires a closed path in polarization state space, which can be achieved using a simple Michelson interferometer and quarter-wave plates, as shown in figure 3 [17].

A polarized laser beam is split into a reference beam A_0 and a beam to be modified A. The latter passes through a quarter-wave plate, creating circular polarization B. This passes through a second quarter-wave, oriented at an angle $\frac{1}{2}\alpha$ relative to the linearly polarized source, which changes the circularly polarized light back to linearly polarized light C, now at some angle relative to the original linearly polarized source A. The linearly polarized beam reflects off the mirror. The second quarter-wave plate now makes C into circularly polarized light D, which has the opposite chirality of B. The first quarter-wave plate returns the light to A, and it interferes with the reference beam A_0.

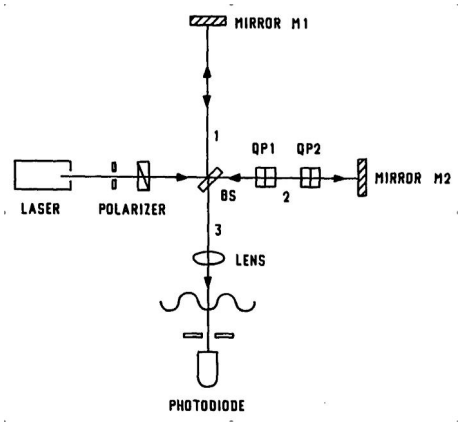

Figure 3: Experimental setup of Mandel *et al.* to observe the Pancharatnam geometric phase. [17]

Rotating the second quarter-waveplate and measuring the resulting interference fringes allows one to measure Pancharatnam's phase. The path enclosed on the Poincaré sphere is $ABCDA$, which has a solid angle Ω of 2α, as shown in figure 4. The Pancharatnam phase Φ_g is therefore α. The data of Mandel *et al.* are in excellent agreement with this.

This experiment by Mandel *et al.* does not account for the dynamical phase, which would manifest as a shift in the interference fringes from instability of the interferometer. A later experiment by Hariharan and Roy [18] eliminates the dynamic phase by using a Sagnac-like interferometer, where both the reference and polarization-modified beams travel along the

same path in opposite directions. A geometric phase is introduced into both beams, and their interference reveals twice the geometric phase in the Mandel *et al.* experiment.

4.2 Spin-redirection geometric phase

The spin-redirection geometric phase rotates the plane of polarized light by adiabatically changing a system in parameter space [19, 20]. To observe this geometric phase, we create an effective optical activity by moving the wavevector $\vec{k}$ on a closed circuit in momentum space.

An optically active material has some chiral property of its molecules, crystal planes, etc. that causes a circularly polarized beam whose chirality does not match that of the material to be affected differently than ones that does. This results in two indices of refraction for different circular polarization states. Birefringence in linearly polarized light is the more familiar analog, where different components of the electric field vector of a linearly polarized light beam experience different indices of refraction.

One way to change $\vec{k}$ adiabatically in momentum space is to send polarized light through a coiled single-mode optical fiber. The wavevector must stay parallel to the local axis of the fiber, which can vary on a scale larger than the order of the wavevector. The geometric phase Φ_g is then given by the solid angle Ω enclosed by the transit of $\vec{k}$ in momentum space:

$$\Phi_g(C) = -\sigma\Omega,$$

where

$$\Omega(C) = 2\pi N(1 - \cos\theta).$$

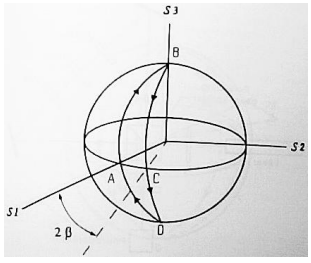

Figure 4: Path on Poincaré sphere that demonstrates the Pancharatnam geometric phase. [17]

Here, the helicity quantum number is $\pm\sigma$, C is the closed path in momentum space, N is the integer number of windings in the helical optical fiber.

Consider a beam of linearly polarized light coupled into a single-mode optical fiber that is wound in a helix, with winding number N, radius r, pitch length d and pitch angle θ, as in figure 5 [20]. (We use linearly polarized light to simplify the experimental setup; helical polarization states form a complete basis so this is entirely acceptable.) For $N = 1$, Berry's phase becomes

$$\Phi_g = -2\pi\sigma \left(1 - \frac{d}{\sqrt{d^2 + (2\pi r)^2}}\right).$$

The initial polarization state that is coupled into the fiber is

$$|x\rangle = \frac{1}{\sqrt{2}}(|+\rangle + |-\rangle),$$

where $|\pm\rangle$ the eigenstates of the helical eigenstate. The state upon exiting the fiber includes the geometric phase term:

$$|x'\rangle = \frac{1}{\sqrt{2}}(e^{\imath\Phi_g}|+\rangle + e^{-\imath\Phi_g}|-\rangle).$$

Malus's law requires the intensity of polarized light transmitted through an analyzing polarizer set an an angle γ is $I_0 \cos^2\gamma$, where I_0 is the square of the electric field amplitude. We see that $\langle x|x'\rangle$ gives a similar result:

$$|\langle x|x'\rangle|^2 = \cos^2\Phi_g.$$

This means that the angle by which the polarization has been rotated is given exactly by Berry's phase Φ_g. This can easily be measured using an analyzing polarizer at the exit of the fiber. An interesting aspect of this experiment is that it must be done in three dimensions to have the desired topological effects [20].

4.3 Transverse laser mode geometric phase

The Pancharatnam and spin-redirection geometric phases deal with the electric field vector of light. Another geometric phase can be found by studying the phase of first-order Gaussian

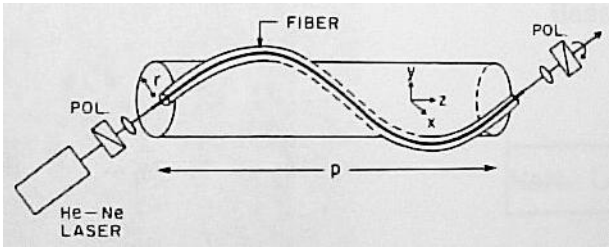

Figure 5: Experimental setup of Tomita and Chiao to measure the spin-redirection geometric phase. [20]

beams [16, 22].

4.3.1 Hermite-Gaussian and Laguerre-Gaussian modes

There exist solutions to the paraxial wave equation beyond the familiar Gaussian function, two examples being Hermite-Gaussian (HG) modes and Laguerre-Gaussian (LG) modes. HG modes have rectangular symmetry, LG modes cylindrical symmetry [23, 24].

The electric field amplitude of the HG mode is described by the Hermite polynomials H of order n and m,

$$HG_{nm}(x, y, z) \propto H_n\left(\frac{\sqrt{2}x}{w}\right) H_m\left(\frac{\sqrt{2}y}{w}\right) e^{\frac{x^2+y^2}{w^2}}$$

The intensity distribution of an HG_{11} beam is four bright lobes arranged in a 2x2 grid and separated by dark lines of zero intensity, as in figure 6. The phase of these lobes alternate between 0 and π.

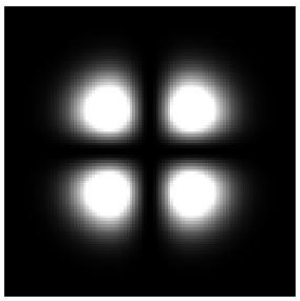

Figure 6: Intensity distribution of Hermite-Gaussian mode $HG_{n=1,m=1}$.

The electric field amplitude of the LG mode is described by the Laguerre polynomials L of order ℓ and p.

$$LG_p^\ell(r,\phi,z) \propto L_p^\ell\left(\frac{2r^2}{w^2}\right) r^\ell e^{\frac{r^2}{w^2}} e^{-\imath\ell\phi}$$

The intensity distribution of an LG beam with indices $p = 1$, $\ell = 1$ is a central bright spot surrounded by a dark ring, then a bright ring (a bull's-eye). More interesting are the LG beams where $p = 0$. These are termed optical vortices because the phase of the beam varies azimuthally, as is evident in the $e^{\imath\ell\phi}$ term of the electric field. This creates a singularity along the axis of the beam where the phase is undefined, and therefore the intensity must go to zero. The result is a ring-shaped beam with a dark core, as in figure 7. Optical vortices form a large part of the exciting and diverse field of singular optics, whose foundation is often credited to Nye and Berry [25, 26, 27].

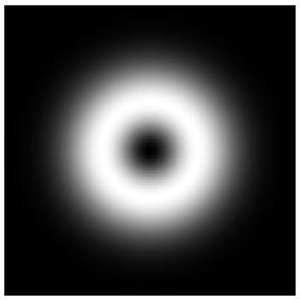

Figure 7: Intensity distribution of Laguerre-Gaussian mode $LG_{p=0}^{\ell=1}$.

The LG modes can decomposed into the sum of HG modes of various orders. For example,

$$LG_0^1 = HG_{10} + \imath\, HG_{01}.$$

Experimentally, this is accomplished using an astigmatic mode converter, which employs two cylindrical lenses to introduce a Guoy phase shift in an HG beam. For HG to LG conversion, a phase shift of of $\frac{\pi}{2}$ is required. An LG_0^{+1} mode can be transformed into a LG_0^{-1} mode by a pair of cylindrical lenses aligned in a different way to give a Guoy phase shift of π

An LG beam can also be made using a "fork" diffraction grating. This is the calculated interference between a Gaussian beam and an off-axis Laguerre-Gaussian beam, which is then transferred to film or written to a programmable or static phase element. A Gaussian

beam incident on the fork grating creates a diffraction pattern where non-zero diffraction orders contain LG beams of increasing ℓ.

What makes these modes so special is their phase. The intensity distribution of the interference between coaxial Gaussian and Laguerre-Gaussian beams is a spiral, with the number of arms equal to ℓ. The interference between two Laguerre-Gaussian beams of equal and opposite ℓ-values is petal-like fringes, with the number of azimuthal lobes equal to 2ℓ.

4.3.2 Poincaré sphere for first-order Gaussian modes

An analog of the Poincaré sphere for polarization states can be constructed for first-order Gaussian beams [12]. The north pole of this mode space is an LG_0^{+1} mode, the south pole LG_0^{-1}, and points along the equator are HG_{10} to HG_{01}. Using the Poincaré model of first-order Gaussian modes, we can easily devise a scheme where varying the parameters of the system create a closed path on the surface of the Poincaré sphere. Two pairs of π converters at an angle α relative to each other create a closed path in mode space separated by $\phi = 2\alpha$. This angle 2α is the geometric phase, which physically corresponds to a phase shift in the LG beam's wavefront.

Figure 8: The Poincaré sphere representation of LG and HG states. [12]

4.3.3 Experiment

The first experiment to observe the geometric phase in first-order Laguerre-Gaussian modes predicted by van Enk [16] was done by Galvez [22]. It requires a closed path on the Poincaré sphere in modespace, and special care to account for the dynamic phase.

At point A on the Poincaré sphere we begin with an LG_0^{-1} beam. It is sent through a $\frac{\pi}{2}$ mode converter and becomes a HG_{01} beam, at point B along the equator. This HG_{01} beam

is rotated by a tunable Dove prism by an angle $\frac{1}{2}\alpha$, which translates the beam along the equator by an angle 2α to point C. Another $\frac{\pi}{2}$ mode converter transforms the HG beam back into an LG_0^1 beam, point A. This second $\frac{\pi}{2}$ mode converter must be aligned with the axis of the Dove-prism-rotated HG beam, so it is set at an angle θ relative to the first $\frac{\pi}{2}$ mode converter.

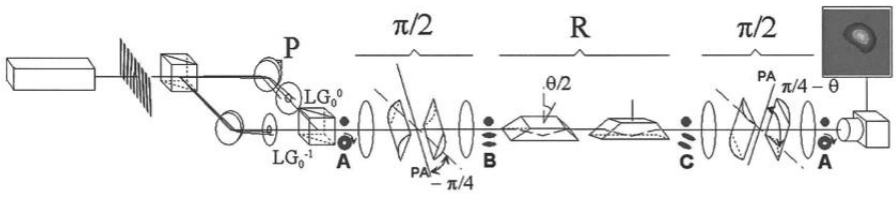

Figure 9: Experimental setup of Galvez *et al.*. [22]

The solid angle Ω enclosed by the path $ABCA$ is 2α, and therefore the geometric phase Φ_g is α. The rotation of the second $\frac{\pi}{2}$ mode converter is thus what controls the amount of geometric phase accumulated by the beam during its transit through the system.

The geometric phase in the case of first-order modes is manifested as an advance in the phasefront of the LG beam. Thus to observe it, the beam must be interfered with a reference beam. The result is a bright lobe located at some azimuthal angle ϕ that changes with the magnitude of the geometric phase Φ_g. Experimentally, interferometers are extremely sensitive due to instabilities that introduce an unwanted dynamic phase. A dynamic phase is normally manifested as the change in path length of one beam relative to the other, causing a shift in interference fringes. The reference Gaussian beam is therefore sent through the entire system collinear with the transforming first-order mode to introduce the same dynamic phase to both beams, rendering it irrelevant.

The mode transformation given by $ABCA$ gives a geometric phase Φ_g equal exactly to the rotation angle α of the second $\frac{\pi}{2}$ mode converter. To measure Φ_g, the angle of the second $\frac{\pi}{2}$ converter is varied, and the azimuthal position of the interference fringe is measured. Galvez's experiment found $\Phi_g = \alpha$, in agreement with theory.

A second experiment was performed by Galvez to further illustrate the geometric phase. At point A on the Poincaré sphere we again begin with an LG_0^{-1} beam, but this time it is sent through a π mode converter. This transforms it into an LG_0^{+1} beam at point D. This beam is returned to its initial state at point A by sending it through a second π mode converter, which is rotated by an angle α. It is this angle that determines the magnitude of geometric

phase acquired. To reveal the geometric phase, the LG beam is again interfered with a Gaussian reference beam. Now the solid angle Ω enclosed by the circuit on the Poincaré sphere is twice what it was before; the geometric phase Φ_g is 2α.

5 Applications of geometric phase

While geometric phase may seem an esoteric subtlety of physics, it does have some applications.

5.1 Polarization rotator

An application of the geometric phase in optics is the rotation of linearly polarized light [28, 29]. A common way to achieve this experimentally is using a half-wave plate, a birefringent transparent material such as quartz. A waveplate must be engineered for a specific wavelength of laser light, both in its physical thickness and its antireflection coatings. Waveplates can be damaged when used with high-power lasers, and are expensive to replace; a high-quality wavelplate can cost hundreds of dollars. Koch and his colleagues pursued using the geometric phase to replace waveplates in their work on Rydberg atoms that uses extremely high-power CO_2 lasers Employing the geometric phase, Koch et. al used mirrors mounted in a closed three-dimensional circuit to rotate the polarization of a laser beam by a desired amount, as in figure 10. The angle by which the polarization is rotated ϕ is equal to the solid angle Ω of the circuit traversed in k-space.

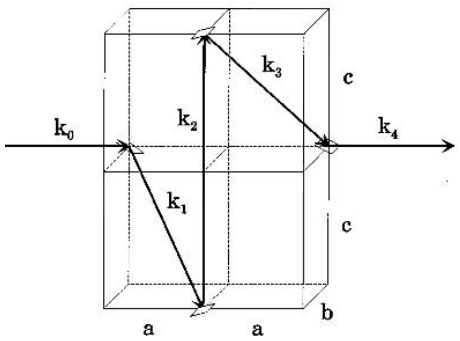

Figure 10: Experimental setup of Koch and Galvez. [29]

6 Summary and Acknowledgments

We have explored the geometric phase in a variety of systems and from a variety of viewpoints. The geometric phase is rooted in the topological evolution of a system. This topic continues to be a popular and insightful one to study in every area of physics.

I would like to thank Prof. Sir Michael Berry for a series of amazing talks and personal discussions in 2005, for having a remarkable vision of physics and math, and for his admiration for others' work as seen in [2]; Prof. Kiko Galvez for innumerable discussions, lab tours and warm encouragement; Stephen Choi, Sung Jong Woo, Kevin Wright, Andrew Kowalik and Prof. Nick Bigelow for many life-changing discussions of Berry's phase in Bose-Einstein condensates; Prof. Alfred Goldhaber for many helpful discussions and suggestions, and the opportunity to write this paper; Prof. Peter Koch for helping "fuel the fire;" Dr. John Noé for book-borrowing and debugging; Todd Gelbord for help learning the joy of fiber bundles; Nick Zachariou for a recommendation of an amazing LaTeX compiler for Mac.

References

[1] M.V. Berry, "Quantal phase factors accompanying adiabatic changes." Proceedings of the Royal Society of London A **392** 45 (1984)

[2] M.V. Berry, "Anticipations of the geometric phase." Physics Today **43**, 34 (1990)

[3] D.J. Griffiths, *Introduction to Quantum Mechanics.* Pearson, 2nd Ed. 2005

[4] J.H. Hannay, "Angle Variable Holonomy in Adiabatic Excursion if an Integrable Hamiltonian." Journal of Physics A **18**, 221 (1985)

[5] Y. Aharonov and D. Bohm, "Significance of electromagnetic potentials in quantum theory." Physical Review Letters **115**, 485 (1959)

[6] P. Kim et al., "Experimental observation of the quantum Hall effect and Berry's phase in graphene." Nature **438**, 201 (2005)

[7] K. Symon, *Mechanics.* Addison-Wesley, 2nd Ed. 1960

[8] D. Chruscinski and A. Jamiolkowski, "Geometric Phases in Classical and Quantum Mechanics." Birkhauser, Progress in Mathematical Physics **36** (2004)

[9] T. Gelbord, "The Aharonov-Bohm Effect." 2006

[10] T. Frangsmyr and G. Ekspang (eds), *Nobel Lectures, Physics 1981-1990.* World Scientific. 1993

[11] S. Pancharatnam, "Generalized theory of interference, and its applications." The Proceedings of the Indian Academy of Sciences A **44**, 247 (1956); reprinted in A. Shapere and F. Wilczek. *Geometric Phases in Physics.* World Scientific. 1989.

[12] M. Born and E. Wolf, *Principles of Optics.* Cambridge University Press, 7th Ed. 1999

[13] M.J. Padgett and J. Courtial, "Poincaré-sphere equivalent for light beams containing orbital angular momonetum." Optics Letters **24**, 430 (1999)

[14] P.W. Milloni and J.H. Eberly, *Lasers.* Wiley. 1988

[15] H. Metcalf and P. van der Straten, *Laser Cooling and Trapping.* Springer. 1999

[16] M.V. Berry, "The adiabatic phase and Pancharatnam's phase for polarized light." Journal of Modern Optics **34**, 1401 (1987)

[17] S.J. van Enk, "Geometric phase, transformations of Gaussian light beams and angular momentum transfer." Optics Communications **102**, 58 (1993)

[18] L. Mandel, R. Simon *et al.*, "Measurement of the Pancharatnam phase for a light beam." Optics Letters **13**, 562 (1988)

[19] P. Hariharan and M. Roy, "A geometric-phase interferometer." Journal of Modern Optics **39**, 1811 (1992)

[20] R. Chiao and Y.-S. Wu, "Manifestations of Berry's Topological Phase for the Photon." Physical Review Letters **57**, 933 (1986)

[21] A. Tomita and R. Chiao, "Observation of Berry's Topological Phase by Use of an Optical Fiber." Physical Review Letters **57**, 937 (1986)

[22] A. Joshi, A.K. Pati and A. Banerjee, "Geometric phase with photon statistics and squeezed light for the dispersive fiber." Physical Review A **49**, 5131 (1994)

[23] E.J. Galvez *et al.*, "Geometric Phase Associated with Mode Transformations of Optical Beams Bearing Orbital Angular Momentum." Physical Review Letters **90**, 203901 (2003)

[24] L. Allen *et al.*, "Orbital angular momentum of light and the transformation of Laguerre-Gaussian laser modes." Physical Review A **45**, 8185 (1992)

[25] L. Allen, *et al.*, "An experiment to observe the intensity and phase structure of LaguerreGaussian laser modes." American Journal of Physics **64**, 77 (1996)

[26] J.F. Nye and M.V. Berry, "Dislocations in wave trains." Proceedings of the Royal Society of London A **336**, 165 (1974)

[27] L. Allen, S.M. Barnett, M.J. Padgett (eds), *Optical Angular Momentum.* Taylor and Francis. 2003

[28] G.A. Swartzlander Jr. (ed), *Vortex Phenomena.* CRC. 2008

[29] L.L. Smith and P.M. Koch, "Use of four mirrors to rotate linear polarization but preserve input-output collinearity." Journal of the Optical Society of America A **13**, 2102 (1996)

[30] E.J. Gavlez and P.M. Koch, "Use of four mirrors to rotate linear polarization but preserve input-output collinearity: II." Journal of the Optical Society of America A **14**, 3410 (1997)